Front. Struct. Civ. Eng. 2022, 16(1): 117–130
https://doi.org/10.1007/s11709-021-0788-7

RESEARCH ARTICLE

Variability of waste copper slag concrete and its effect on the seismic safety of reinforced concrete building: A case study

Swetapadma PANDA[a,b*], Nikhil P. ZADE[b], Pradip SARKAR[b], Robin DAVIS[c]

[a] *Department of Civil Engineering, Institute of Technical Education and Research, Odisha 751 030, India*
[b] *Department of Civil Engineering, National Institute of Technology Rourkela, Odisha 769 008, India*
[c] *Department of Civil Engineering, National Institute of Technology Calicut, Kerala 673 601, India*
[*] *Corresponding author. E-mail: swetapadma.nit2017@gmail.com*

ABSTRACT Proven research output on the behavior of structures made of waste copper slag concrete can improve its utilization in the construction industry and thereby help to develop a sustainable built environment. Although numerous studies on waste copper slag concrete can be found in the published literature, no research has focused on the structural application of this type of concrete. In particular, the variability in the strength properties of waste copper slag concrete, which is required for various structural applications, such as limit state design formulation, reliability-based structural analysis, etc., has so far not attracted the attention of researchers. This paper quantifies the uncertainty associated with the compressive-, flexural- and split tensile strength of hardened concrete with different dosages of waste copper slag as fine aggregate. Best-fit probability distribution models are proposed based on statistical analyses of strength data generated from laboratory experiments. In addition, the paper presents a reliability-based seismic risk assessment of a typical waste copper slag incorporated reinforced concrete framed building, considering the proposed distribution model. The results show that waste copper slag can be safely used for seismic resistant structures as it results in an identical probability of failure and dispersion in the drift demand when compared with a conventional concrete building made of natural sand.

KEYWORDS waste copper slag, quantification of variability, goodness-of-fit test, seismic risk assessment, PSDM

1 Introduction

Managing industrial waste through recycling is the best way to protect environmental health and conserve natural resources. The utilization of industrial waste as supplementary raw material in concrete production contributes towards efficient waste minimization [1–9]. Furthermore, the use of industrial waste in concrete compensates for the lack of natural resources and safeguards nature. Efficient substitute materials to fine aggregates, like iron slag, waste foundry sand, waste copper slag (WCS), imperial smelting furnace slag, etc., in concrete production, have been carried out for over a decade now [3,4]. Among them, WCS is found to be pozzolonically active industrial waste and can produce ultrahigh performance concrete [10]. Many investigators [11–14] have also tried to use WCS as supplementary cementitious material in concrete making. However, the physico-chemical properties of WCS, generated during the smelting and pyrometallurgical extraction of copper from its ore, are found to offer a fine aggregate that is superior to natural sand, for several reasons [15–24]. It is reported [16,19,21] that WCS can be effectively utilized as a substitute for natural sand to acquire mortar and concrete of good strength and durability. The positive impact of utilizing WCS as a substitute for natural sand on the physical, chemical, and mechanical properties of high-strength concrete have been reported in published literature [10]. Up to 40% replacement of natural sand with WCS can accomplish a concrete strength better than the control blend [17] due to the superior compressibility of WCS which partially mitigates the stress concentration. Despite

Article history: Received Jul 20, 2021; Accepted Oct 18, 2021

such research efforts, the practical use of WCS in concrete construction has not been satisfactorily finalized. Therefore, design and safety of WCS incorporated concrete structures need due focus in order to help improve practical use.

Limit state design philosophy is widely used for the design of reinforced concrete (RC) structures. The partial safety factor for the strength of materials used in the limit state design depends on the characteristic values of material strength, its dispersion, and the probability distribution [25]. Similarly, variability in the strength properties influences the risk or safety assessment of any structure. Experimental evaluations of the probability distribution of strength parameters for common structural materials (e.g., conventional concrete, steel reinforcement) have been reported in the literature. Compressive strength data of concrete cores are statistically characterized to recommend the probability distribution function for describing variability [26]. Variability analysis for compressive- and split tensile strength for conventional concrete has been studied by many investigators [27–34]. Multiple statistical norms and several distribution functions were developed to categorize the variability analysis of compressive strength of concrete by Chen et al. [31]. Such studies for conventional concrete may not be appropriate for correctly assessing the variability of WCS concrete as the inherent properties of WCS and natural sand are not alike. Although a significant variation in the strength properties of the WCS concrete are reported in the published literature, no research attempt has been found to transform these variations into a statistical distribution which is essential for the formulation of the limit state/reliability-based design of WCS concrete structures. Furthermore, all past research on WCS concrete has focused primarily on material testing for strength and durability, ignoring the issue of associated structural behavior.

Therefore, the present study investigates the variability associated with structural concrete made with WCS as an alternative to natural sand. Strength properties of WCS concrete were experimentally evaluated and probability distribution functions that fit the experimental data best were recommended. A systematic performance assessment of structure made of WCS can determine the acceptability for its practical use, which formed an important motivation of the present paper. Accordingly, a case study of probability-based seismic risk assessment was conducted for a selected RC-framed building made of WCS concrete, considering the experimentally obtained material properties and recommended variability models.

2 Research significance

The actual usage of WCS concrete at the construction site is low, even though several published literatures have confirmed that WCS can be used as a replacement of natural sand in concrete construction. This may be due to the lack of available research output on the aspects of design and safety of WCS-incorporated concrete structures. All of the past studies on WCS concrete are based only on material testing in terms of strength and durability. This paper is the first attempt to evaluate and report the variability of different strength properties of WCS concrete necessary for the formulation of the limit state/reliability-based design of WCS concrete structures. In addition, this paper investigated the seismic risk of a typical building made of WCS concrete and reports that the WCS can be safely utilized for seismic resistant structures.

3 Experimental programme

The primary objective of this work is to conduct a seismic risk assessment of a typical RC framed building made using WCS. The probability-based seismic risk assessment methodology requires consideration of uncertainty in loading and strength of the structure. The variability models of conventional concrete available in past literature may not be suitable for WCS concrete as WCS poses different material characteristics in comparison with natural sand. Hence, this section focuses on the uncertainty quantification of the strength properties of WCS concrete through an experimental program and proposes the most appropriate distribution functions to describe the variability in considered strength parameters. Compressive-, flexural-, and split tensile strengths are considered here as representative strength parameters of WCS concrete. The WCS used in the present study was collected from only one source: the Indian copper complex at Ghatsila, a refinery of Hindustan Copper Ltd. (India). Portland cement of 43 grade conforming to ASTM C150 [35], the coarse aggregate of angular grades with a nominal size of 20 mm and natural sand conforming to ASTM C33 [36] were used along with WCS for the preparation of concrete specimens. Further details about the Physico-chemical properties of sand and WCS are given in Table 1 and also found in available literature [37].

The experimental program considered a mix design as reported in published literature [37]. Six different concrete mixes were prepared by partial or full replacement of natural sand with WCS and designated as M0, M20, M40, M60, M80, and M100, respectively, where ‘M’ presents the mix and number denotes the volumetric percentage replacement of natural sand with WCS. Table 2 gives the mixture proportions considered in this study.

Concrete cubes of 150 mm, prisms of 100 mm × 100 mm ×

700 mm, and cylinders of 150 mm diameter × 300 mm height were cast following ASTM C192 [38] from each of the six WCS concrete mixes for compressive-, flexure- and split tensile strength tests respectively. Compressive-, flexure- and split tensile strengths of WCS concrete were evaluated experimentally after 28 days of water curing following the guidelines of IS 516 [39], ASTM C496 [40], and ASTM C293 [41], respectively. Photographs of typical test specimens are shown in Fig. 1.

4 Variability assessment

Thirty specimens for each of the six mixes (a total of 180 specimens) were tested under each of the three selected strength categories. Table 3 presents the mean, standard deviation (SD), and range of strength properties obtained from the experimental results. The three selected strength properties of WCS concrete were found to be enhanced by increasing the dose of WCS content up to 80%. This result supports the conclusions of some of the earlier studies on WCS concrete [37]. Better grading of WCS than of natural sand results in better concrete strength through improved particle packing; also the presence of Class-N pozzolana in WCS can help achieve better concrete strength [37].

When the WCS proportion is greater than 80%, the free water in the cement matrix increases considerably due to the low water absorption capacity of the WCS, which causes an increase in voids and, consequently, a decrease in the strength of hardened WCS concrete. The observed mean values of compressive-, flexural-, and split tensile strength of WCS concrete are shown in Figs. 2(a), 2(b), and 2(c), respectively.

The variability in any strength property needs to be expressed in terms of a statistical distribution to be used for probability-based structural analysis. Therefore, experimentally obtained results were analysed using four non-parametric goodness-of-fit (GOF) tests: Kolmogorov-Smirnov (KS), Kolmogorov-Smirnov-Lilliefors (KSL), Anderson-Darling (AD), and Chi-Square (CS) and the best-fit statistical distributions for each of the three selected strength parameters were evaluated. The methodology of all GOF tests is to measure the difference between the observed and the theorized cumulative distribution function (CDF), which is known as the

Table 1 Physico-chemical properties of fine aggregates

material	physical property				chemical property			
	fineness modulus	relative density (kg/m^3)	water absorption (%)	co-efficient of uniformity	$SiO_2 + Al_2O_3 + Fe_2O_3$ (% by mass)	MgO (% by mass)	SO_3 (% by mass)	CaO (% by mass)
sand	4.68	3.89	0.36%	3.05	92.23	1.89	1.45	1.05
WCS	2.89	2.6	0.80%	2.32	58.15	–	–	0.48

Table 2 Details of selected WCS concrete mixes

component	M0	M20	M40	M60	M80	M100
WCS replacement by volume (% of sand)	0	20	40	60	80	100
cement (kg/m^3)	450	450	450	450	450	450
natural sand (kg/m^3)	608	486.4	364.8	243.2	121.6	0
WCS (kg/m^3)	0	177	353	530	706	883
coarse aggregate (kg/m^3)	1215	1215	1215	1215	1215	1215
water (kg/m^3)	180	180	180	180	180	180

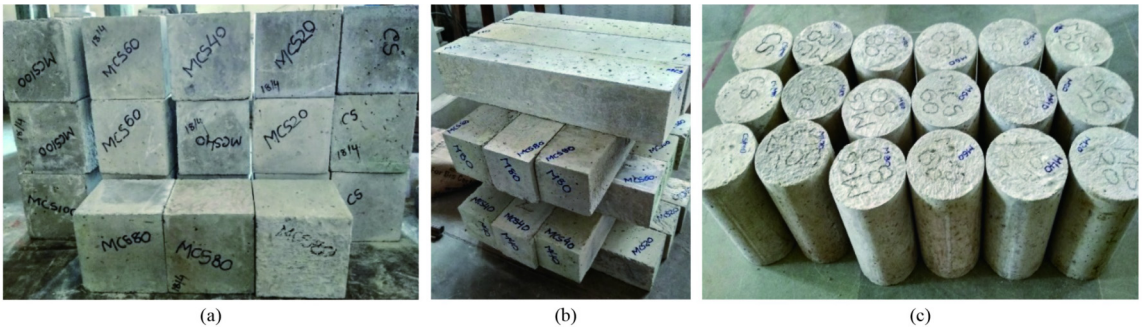

(a) (b) (c)

Fig. 1 WCS concrete specimens for evaluation of strength properties. (a) Cubes for compressive strength; (b) prisms for flexural strength; (c) cylinders for split tensile strength.

'statistic'. It should be noted that a lower 'statistic' value indicates a smaller difference between the actual and the theorized CDF, and therefore a better performance of the chosen distribution in the variability modelling. The 'statistic' value must be lower than a 'critical' value corresponding to the selected significance level. The estimations of the 'statistic' and the associated 'critical' values differ in different GOF tests. The KS test does not depend on sample size and performs better for continuous distributions. The KSL and KS are identical in terms of the statistic but different in terms of the critical values [42]. However, both of these two tests are sensitive near the middle of the distribution than at the tails [43]. AD is a modified version of the KS test which is more sensitive to the tail region [44]. The CS test is more efficient when a large number of random variables are used.

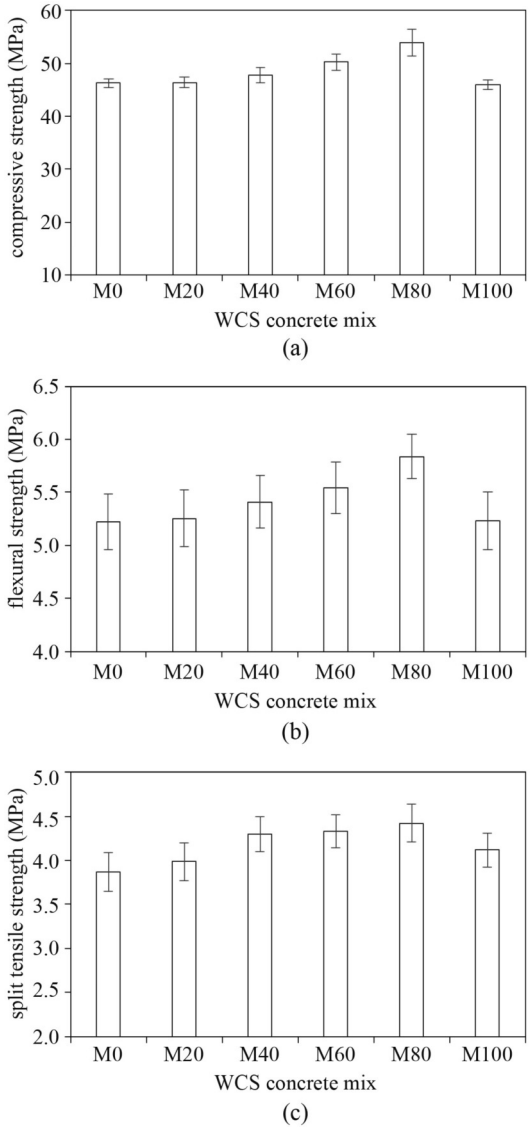

Fig. 2 Mean strength of concrete versus WCS replacement. (a) Compressive strength; (b) flexural strength; (c) split tensile strength.

Two-parameter probability distribution functions are assumed to be representative of the variability of strength properties of WCS concrete. Six two-parameter distribution functions, those previously proven [45–49] to be useful in modelling the strength properties of brittle materials, were selected in the present study. Detailed formulations of the selected distribution functions are available in the published literature [50]. The test statistic was determined for each of the selected distribution function and ranked based on the statistic value. For each probability distribution function, the test statistic was determined and ranked. Commercial software EasyFit Professional [51] was used for all the statistical analyses. Tables 4–6 present the location, shape, and scale parameters of selected distribution functions estimated from the experimental results.

Similarly, Figs. 3–5 present the CDF of the selected distribution functions along with the experimental data. Tables 7 to 9 present the statistic values for each of the selected probability distributions obtained from the GOF tests and the corresponding rankings based on their statistic values for compressive, flexural and split tensile strength data.

It can be observed from Tables 7 to 9 that the selected GOF test criteria (KS/KSL, AD, and CS) do not agree with one single probability distribution for modelling the variability of strength properties of WCS concrete. For example, KS/KSL and AD ranked the normal distribution as the best-fit variability model for compressive strength whereas CS ranked Gumbel max as the best fit for the same strength property as shown in Table 7. Similarly, multiple distributions were ranked as the best-fit

Table 3 Strength properties of WCS concrete

specimen	compressive strength (MPa)			split tensile strength (MPa)			flexural strength (MPa)		
	mean	SD	range	mean	SD	range	mean	SD	range
M0	46.3	0.79	45.0–47.9	3.87	0.22	3.6–4.2	5.22	0.27	4.9–5.6
M20	46.4	0.99	45.9–48.5	3.39	0.21	3.6–4.3	5.26	0.27	4.9–5.6
M40	47.8	1.48	46.1–50.7	4.30	0.20	3.9–4.5	5.41	0.24	5.0–5.7
M60	50.2	1.48	48.1–52.5	4.33	0.19	4.0–4.7	5.54	0.24	5.1–5.8
M80	53.9	2.56	50.0–57.0	4.42	0.22	4.1–4.8	5.84	0.21	5.3–5.9
M100	46.0	0.94	44.4–47.8	4.12	0.19	3.8–4.4	5.23	0.21	4.9–5.7

Table 4 Parameters of probability distribution functions for compressive strength (MPa)

distribution	parameter					
	M0	M20	M40	M60	M80	M100
normal	μ = 46.25 σ = 0.79	μ = 46.41 σ = 0.99	μ = 47.81 σ = 1.48	μ = 50.23 σ = 1.47	μ = 53.86 σ = 2.56	μ = 46.01 σ = 0.94
lognormal	μ = 3.83 σ = 0.02	μ = 3.83 σ = 0.02	μ = 3.866 σ = 0.03	μ = 3.916 σ = 0.03	μ = 3.98 σ = 0.05	μ = 3.82 σ = 0.02
Gamma	α = 3416.7 β = 0.01	α = 2179.5 β = 0.02	α = 1046.4 β = 0.04	α = 1156.0 β = 0.04	α = 442.7 β = 0.12	A = 2415.9 β = 0.02
Weibull	α = 66.61 β = 46.56	α = 52.14 β = 46.81	α = 34.88 β = 48.42	α = 37.32 β = 50.85	α = 22.57 β = 54.99	α = 56.88 β = 46.37
Gumbel max	μ = 45.89 σ = 0.62	μ = 45.96 σ = 0.77	μ = 47.14 σ = 1.15	μ = 49.56 σ = 1.15	μ = 52.71 σ = 1.99	μ = 45.59 σ = 0.73
Gumbel min	μ = 46.60 σ = 0.62	μ = 46.86 σ = 0.77	μ = 48.47 σ = 1.15	μ = 50.89 σ = 1.15	μ = 55.02 σ = 1.99	μ = 46.44 σ = 0.73

Notes: μ: continuous location parameters; α: continuous shape parameters; β, σ: continuous scale parameters

Table 5 Parameters of probability distribution functions for flexural strength (MPa)

distribution	parameter					
	M0	M20	M40	M60	M80	M100
normal	μ = 5.23 σ = 0.26	μ = 5.25 σ = 0.27	μ = 5.41 σ = 0.25	μ = 5.54 σ = 0.24	μ = 5.84 σ = 0.21	μ = 5.23 σ = 0.27
lognormal	μ = 1.65 σ = 0.05	μ = 1.66 σ = 0.05	μ = 1.69 σ = 0.04	μ = 1.71 σ = 0.04	μ = 1.76 σ = 0.03	μ = 1.65 σ = 0.05
Gamma	α = 387.75 β = 0.02	α = 388.56 β = 0.02	α = 490.11 β = 0.01	α = 517.60 β = 0.01	α = 770.97 β = 0.01	α = 377.07 β = 0.02
Weibull	α = 22.31 β = 5.33	α = 22.52 β = 5.36	α = 24.25 β = 5.52	α = 25.64 β = 5.64	α = 31.27 β = 5.93	α = 22.36 β = 5.33
Gumbel max	μ = 5.10 σ = 0.20	μ = 5.13 σ = 0.20	μ = 5.30 σ = 0.20	μ = 5.43 σ = 0.19	μ = 5.74 σ = 0.16	μ = 5.11 σ = 0.21
Gumbel min	μ = 5.34 σ = 0.20	μ = 5.37 σ = 0.20	μ = 5.52 σ = 0.20	μ = 5.65 σ = 0.19	μ = 5.93 σ = 0.17	μ = 5.35 2σ = 0.21

Notes: μ: continuous location parameters; α: continuous shape parameters; β, σ: continuous scale parameters

Table 6 Parameters of probability distribution functions for split tensile strength (MPa)

distribution	parameter					
	M0	M20	M40	M60	M80	M100
normal	μ = 3.87 σ = 0.22	μ = 3.98 σ = 0.21	μ = 4.30 σ = 0.12	μ = 4.33 σ = 0.18	μ = 4.41 σ = 0.20	μ = 4.12 σ = 0.19
lognormal	μ = 1.35 σ = 0.05	μ = 1.38 σ = 0.05	μ = 1.45 σ = 0.04	μ = 1.46 σ = 0.04	μ = 1.48 σ = 0.04	μ = 1.41 σ = 0.04
Gamma	α = 309.88 β = 0.01	α = 355.09 β = 0.01	α = 468.63 β = 0.01	α = 541.77 β = 0.01	α = 467.71 β = 0.01	α = 458.75 β = 0.01
Weibull	α = 19.85 β = 3.95	α = 21.62 β = 4.07	α = 24.36 β = 4.38	α = 26.98 β = 4.40	α = 24.26 β = 4.49	α = 23.83 β = 4.20
Gumbel max	μ = 3.77 σ = 0.17	μ = 3.89 σ = 0.16	μ = 4.21 σ = 0.15	μ = 4.24 σ = 0.14	μ = 4.31 σ = 0.15	μ = 4.03 σ = 0.15
Gumbel min	μ = 3.97 σ = 0.17	μ = 4.08 σ = 0.16	μ = 4.39 σ = 0.15	μ = 4.42 σ = 0.14	μ = 4.50 σ = 0.15	μ = 4.21 σ = 0.15

Notes: μ: continuous location parameters; α: continuous shape parameters; β, σ: continuous scale parameters

variability model for flexural- and split tensile strength by different GOF tests (refer to Tables 8–9). It can also be seen that the best-fit variability model of WCS concrete changed with the change in percentage replacement of WCS. The material characteristics of hardened WCS concrete varied with the percentage replacement of WCS. However, the statistic values of some of the high-ranking distributions were very close. Also, a change in the data pool may alter the ranking of the distributions slightly. Therefore, any of the high-ranking distributions from Tables 7–9 could be used for the structural analysis. A total statistic, which is defined as the square root of the sum of the squares of individual test statistics corresponding to each GOF test, was considered in the present study to select a single best-fit distribution. Table 10 presents the recommended variability models for strength properties of WCS concrete.

It is to be noted here that construction at a practical site may have additional variability arising out of the raw materials obtained from different sources, different

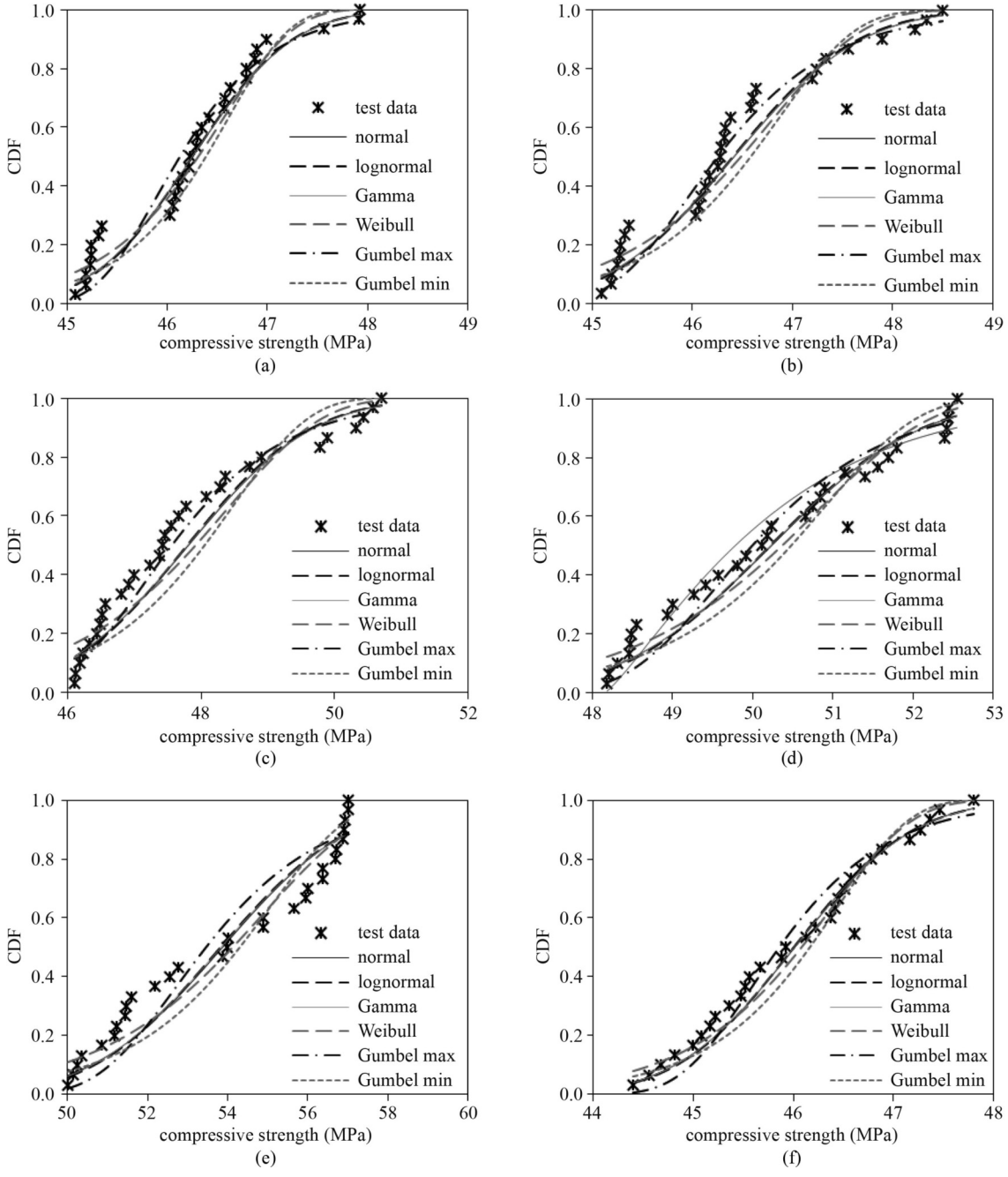

Fig. 3 CDF plot of WCS concrete compressive strength with selected distribution function. (a) M0; (b) M20; (c) M40; (d) M60; (e) M80; (f) M100.

climatic conditions, differences in quality control, etc. which are not included in the present study. In the absence of a comprehensive study, the variability models recommended in Table 10 can be treated as the estimates of the expected variability. A microstructural analysis of WCS concrete may be of importance, especially to understand the reason behind the variability in the strength properties as well as to evaluate the characteristics of the interfacial transition zone in terms of its transport properties and corrosion resistance [52–54]. However, the microstructural characterization remains outside the scope of the present study in order to keep the focus on the statistical modeling of the variability in the strength properties of WCS concrete and its suitability for seismic resistant structures.

5 Seismic response assessment

This section reports on investigation of the seismic performance of a typical RC framed building made of WCS concrete. The purpose of this study was to check

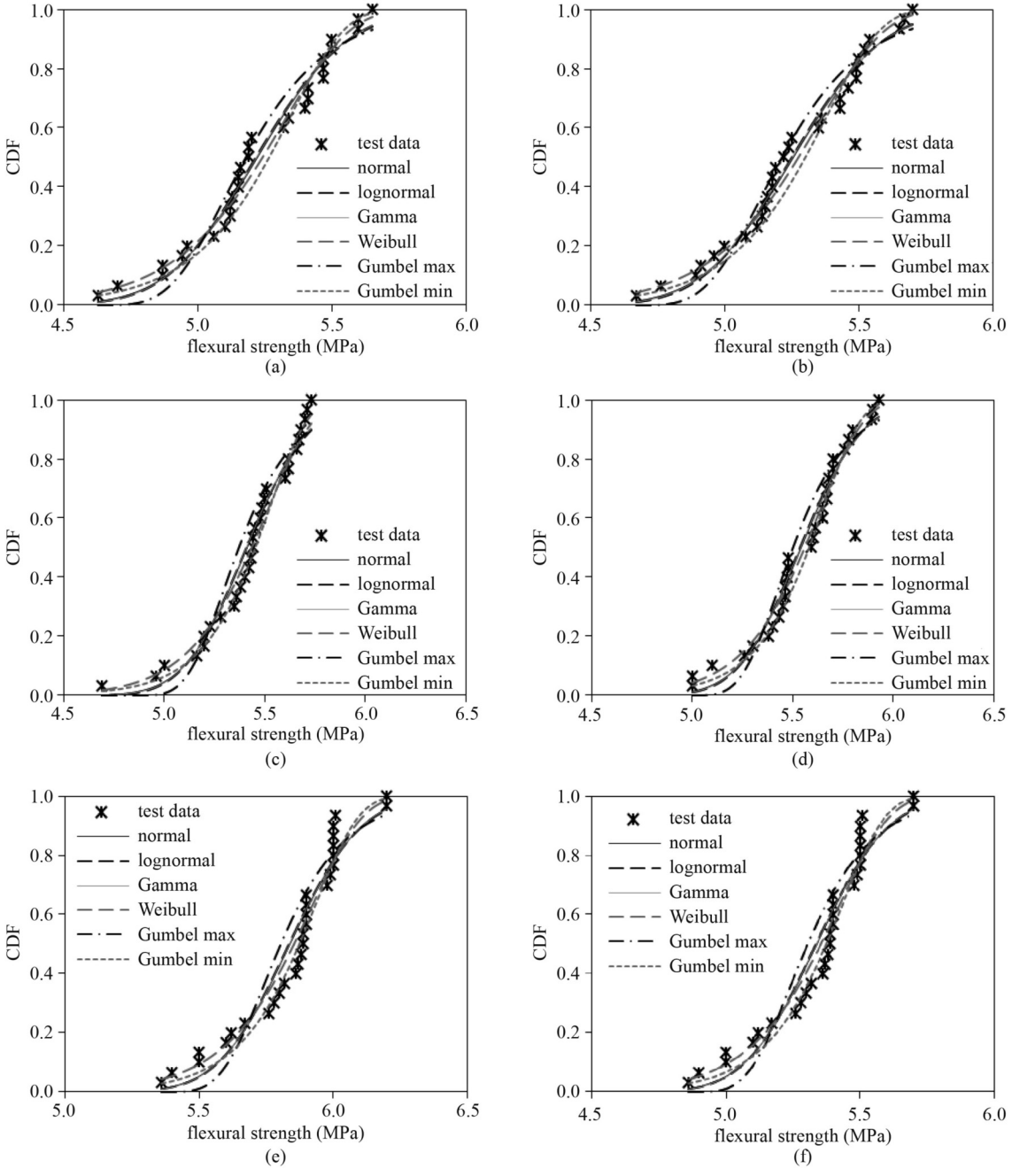

Fig. 4 CDF plot of WCS concrete flexural strength with selected distribution function. (a) M0; (b) M20; (c) M40; (d) M60; (e) M80; (f) M100.

the applicability of the WCS concrete in the seismic-resistant building structure. A probability-based seismic evaluation method [55] using incremental dynamic analysis (IDA) was employed for this purpose. Peak-ground acceleration (PGA) and maximum inter-storey drift (ISD) were considered as ground motion intensity measure (*IM*) and engineering demand parameter, respectively. The seismic performance was evaluated through the probabilistic seismic demand model (PSDM) and fragility curves. The fragility function represents the probability of exceedance of a selected demand parameter beyond the chosen structural limit state at a particular *IM*. It can be expressed in the closed-form [56] as follows:

$$P(C \leqslant D|IM) = \Phi\left(\frac{\ln(\hat{D}) - \ln(\hat{C})}{\sqrt{\beta_{D|IM}^2 + \beta_c^2 + \beta_m^2}}\right), \quad (1)$$

where Φ is the standardized Gaussian CDF, D is the drift demand, C is the drift capacity at a chosen limit state; $\hat{D}$, and $\hat{C}$ are median of demand and chosen limit state, respectively. The values of $\hat{C}$ for the performance level of

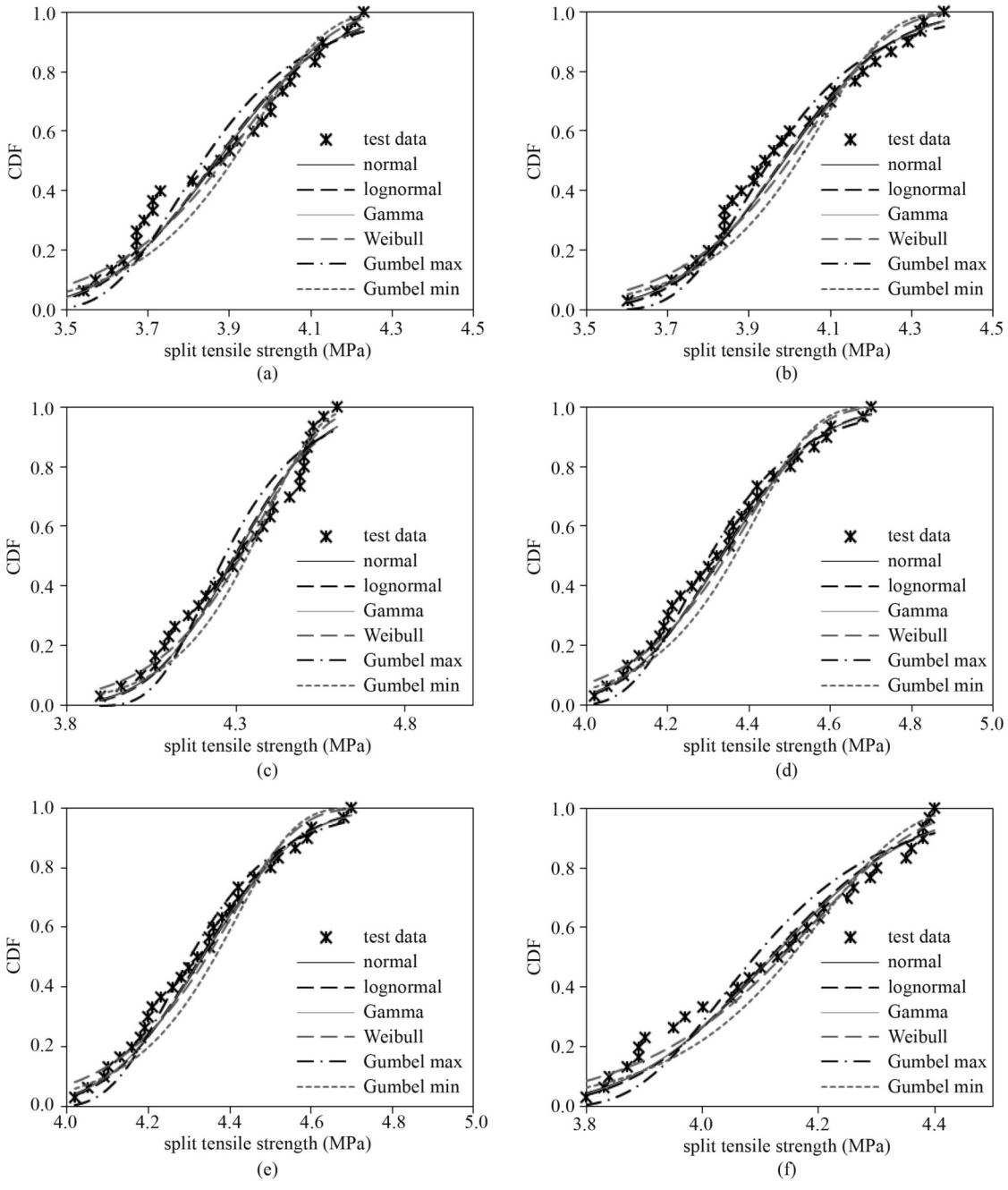

Fig. 5 CDF plot of WCS concrete split tensile strength with selected distribution function.

RC moment-resisting frame are considered from published literature [56–58] as 1%, 2%, and 4%. $\beta_{D|IM}$, β_c, and β_m are the dispersions in intensity measure, capacity, and modeling, respectively. Nonlinear time history analysis (NLTHA) was conducted to obtain maximum ISD, which was the demand parameter considered in the present study. This method used two analytical approximations. The first one was the power-law relationship between median drift demand and the intensity measure [56].

$$\hat{D} = a(IM)^b, \tag{2}$$

where a and b are the constant coefficients. The second approximation was that the drift demand, D is distributed log-normally [55] with a dispersion $\beta_{D|IM}$ about the median. A regression test was performed and a power-law relation (Eq. (2)) was established to obtain a, b, and $\beta_{D|IM}$ from the NLTHA results.

A typical eight-storey four-bay RC framed building (Fig. 6) was considered in the present study with a uniform storey height of 3.5 m and uniform bay width of 5 m. The building was considered to be symmetric in plan and elevation, and a representative central frame was considered for the analysis. The building was designed

Table 7 GOF test results for compressive strength of WCS concrete

mix	distribution	KS/KSL		AD		CS		total statistics	final rank
		stat.	rank	stat.	rank	stat.	rank		
M0	normal	0.142	2	0.653	1	0.045	1	0.669	1
	lognormal	0.147	5	0.674	3	0.066	3	0.693	3
	Gamma	0.142	2	0.653	1	0.050	2	0.670	2
	Weibull	0.110	1	1.012	4	0.920	5	1.372	4
	Gumbel max	0.181	6	1.412	5	2.615	6	2.977	6
	Gumbel min	0.146	4	1.474	6	0.819	4	1.693	5
M20	normal	0.147	3	0.809	4	1.955	2	2.121	2
	lognormal	0.144	1	0.806	3	2.302	3	2.443	3
	Gamma	0.145	2	0.786	2	2.345	4	2.477	4
	Weibull	0.173	5	1.511	5	9.532	6	9.653	6
	Gumbel max	0.152	4	0.780	1	0.297	1	0.848	1
	Gumbel min	0.218	6	2.403	6	8.966	5	9.285	5
M40	normal	0.141	4	1.089	4	3.006	4	3.200	4
	lognormal	0.135	2	1.064	3	1.820	3	2.112	3
	Gamma	0.137	3	1.035	2	1.693	2	1.989	2
	Weibull	0.168	5	1.844	5	3.845	5	4.267	5
	Gumbel max	0.107	1	0.539	1	0.252	1	0.604	1
	Gumbel min	0.211	6	3.264	6	5.004	6	5.978	6
M60	normal	0.106	1	0.620	2	1.950	3	2.049	3
	lognormal	0.111	3	0.650	3	2.049	4	2.153	4
	Gamma	0.106	2	0.608	1	1.934	2	2.030	2
	Weibull	0.125	4	0.849	4	2.848	5	2.974	5
	Gumbel max	0.144	6	0.949	5	1.719	1	1.968	1
	Gumbel min	0.142	5	1.601	6	5.017	6	5.268	6
M80	normal	0.160	2	1.235	2	2.964	1	3.215	1
	lognormal	0.165	4	1.302	4	3.186	3	3.446	3
	Gamma	0.161	3	1.247	3	3.051	2	3.299	2
	Weibull	0.140	1	1.036	1	3.345	4	3.504	4
	Gumbel max	0.195	6	1.984	6	8.148	6	8.388	6
	Gumbel min	0.169	5	1.651	5	4.617	5	4.906	5
M100	normal	0.086	2	0.230	2	0.424	1	0.490	1
	lognormal	0.088	3	0.254	3	0.479	3	0.549	3
	Gamma	0.084	1	0.229	1	0.431	2	0.495	2
	Weibull	0.095	4	0.509	4	0.584	4	0.781	4
	Gumbel max	0.142	6	0.704	5	2.981	6	3.066	6
	Gumbel min	0.139	5	0.841	6	1.437	5	1.670	5

using IS 1893 [59] for seismic load associated with the highest seismic zone of India (with a peak ground acceleration of 0.36g under a maximum magnitude earthquake). Characteristic compressive strength of concrete and characteristic yield strength of reinforcement steel were considered for the design as 40 and 415 MPa, respectively. The dead load of the building included the self-weight of the members, 125 mm thick slab load, and 230 mm thick infill wall load. The imposed load on the floors and roof was considered following the guidelines of IS 1893 [59]. The building models were designed using commercial software SAP 2000 [60]

Table 8 GOF test results for flexural strength of WCS concrete

mix	distribution	KS/KSL		AD		CS		total statistics	final rank
		stat..	rank	stat..	rank	stat..	rank		
M0	normal	0.115	1	0.410	1	0.096	3	0.437	1
	lognormal	0.120	3	0.460	4	0.096	4	0.485	3
	Gamma	0.118	2	0.439	3	0.095	2	0.464	2
	Weibull	0.126	4	0.426	2	2.492	5	2.532	5
	Gumbel max	0.155	5	1.365	6	0.037	1	1.375	4
	Gumbel min	0.171	6	0.635	5	9.142	6	9.166	6
M20	normal	0.109	2	0.290	1	1.803	4	1.830	4
	lognormal	0.115	4	0.331	3	0.099	3	0.364	2
	Gamma	0.112	3	0.312	2	0.098	2	0.346	1
	Weibull	0.104	1	0.367	4	2.601	5	2.629	5
	Gumbel max	0.151	6	1.126	6	0.033	1	1.137	3
	Gumbel min	0.147	5	0.602	5	5.135	6	5.173	6
M40	normal	0.133	3	0.635	3	1.345	5.00	1.493	2
	lognormal	0.142	5	0.737	5	1.319	3.00	1.518	4
	Gamma	0.139	4	0.701	4	1.331	4.00	1.510	3
	Weibull	0.112	2	0.426	2	1.754	6.00	1.808	5
	Gumbel max	0.193	6	2.362	6	1.215	2.00	2.663	6
	Gumbel min	0.091	1	0.274	1	0.463	1.00	0.546	1
M60	normal	0.112	2	0.470	3	0.794	3	0.929	3
	lognormal	0.120	4	0.555	5	0.711	1	0.910	2
	Gamma	0.117	3	0.525	4	0.711	2	0.892	1
	Weibull	0.091	1	0.306	1	2.776	6	2.794	5
	Gumbel max	0.180	6	2.058	6	1.972	5	2.855	6
	Gumbel min	0.133	5	0.324	2	1.158	4	1.210	4
M80	normal	0.172	3	1.001	3	2.094	3	2.327	3
	lognormal	0.180	5	1.093	5	3.163	4	3.352	4
	Gamma	0.177	4	1.059	4	3.752	5	3.903	5
	Weibull	0.143	2	0.730	2	0.523	2	0.910	2
	Gumbel max	0.243	6	2.911	6	6.395	6	7.031	6
	Gumbel min	0.137	1	0.664	1	0.456	1	0.817	1
M100	Normal	0.080	2	0.167	1	0.178	1	0.257	1
	Lognormal	0.090	4	0.192	3	0.195	2	0.288	2
	Gamma	0.086	3	0.178	2	0.198	3	0.280	3
	Weibull	0.078	1	0.366	4	0.472	4	0.602	4
	Gumbel max	0.150	6	0.826	6	3.693	6	3.787	5
	Gumbel min	0.113	5	0.687	5	2.211	5	2.318	6

following the guidelines of IS 456 [61].

Selected buildings were modeled and analyzed using the open-source software Open SEES [62] for NLTHA. A force-based nonlinear beam-column fiber element was used for the modeling of beams and columns, which considered the spread of plasticity along the element. Each element was divided into five integration points. In the present study, uncertainty in loading was considered by selecting 22 pairs (44 ground motions) of far-field ground motions [63]. The details of selected ground motions are also available in the published literature [64]. The uncertainty in the compressive strength of WCS

Table 9 GOF test results for split tensile strength of WCS concrete

mix	distribution	KS/KSL		AD		CS		total statistics	final rank
		stat.	rank	stat.	rank	stat.	rank		
M0	normal	0.138	4	0.478	1	3.079	1	3.119	1
	lognormal	0.135	3	0.523	4	3.230	3	3.275	3
	Gamma	0.134	2	0.487	2	3.122	2	3.162	2
	Weibull	0.134	1	0.522	3	4.466	4	4.499	4
	Gumbel max	0.151	5	1.043	6	4.976	5	5.086	5
	Gumbel min	0.180	6	0.919	5	6.037	6	6.109	6
M20	normal	0.091	3	0.334	3	2.330	4	2.355	4
	lognormal	0.089	2	0.314	2	2.258	2	2.281	2
	Gamma	0.086	1	0.300	1	2.270	3	2.292	3
	Weibull	0.103	5	0.788	5	2.558	5	2.679	5
	Gumbel max	0.096	4	0.395	4	0.110	1	0.421	1
	Gumbel min	0.153	6	1.413	6	4.747	6	4.955	6
M40	normal	0.131	1	0.538	2	1.453	1	1.555	1
	lognormal	0.133	3	0.595	4	1.541	3	1.657	3
	Gamma	0.131	2	0.563	3	1.495	2	1.603	2
	Weibull	0.139	4	0.469	1	3.328	4	3.364	4
	Gumbel max	0.152	5	1.448	6	3.907	5	4.169	5
	Gumbel min	0.153	6	0.702	5	5.450	6	5.497	6
M60	Normal	0.080	2	0.197	3	0.315	2	0.380	1
	lognormal	0.081	3	0.191	2	0.481	4	0.524	4
	gamma	0.078	1	0.177	1	0.422	3	0.464	2
	Weibull	0.089	4	0.657	5	0.725	5	0.982	5
	Gumbel max	0.105	5	0.396	4	0.237	1	0.473	3
	Gumbel min	0.126	6	1.171	6	2.223	6	2.515	6
M80	normal	0.112	4	0.551	4	1.718	2	1.808	2
	lognormal	0.110	3	0.543	3	1.968	4	2.044	4
	Gamma	0.107	2	0.513	2	1.799	3	1.873	3
	Weibull	0.122	5	0.987	5	2.774	5	2.947	5
	Gumbel max	0.100	1	0.487	1	1.129	1	1.233	1
	Gumbel min	0.169	6	1.784	6	5.070	6	5.377	6
M100	normal	0.108	2	0.495	2	2.304	5	2.359	5
	lognormal	0.113	4	0.551	4	2.254	4	2.323	4
	Gamma	0.109	3	0.511	3	2.158	3	2.220	3
	Weibull	0.100	1	0.481	1	1.006	1	1.119	1
	Gumbel max	0.147	6	1.314	6	3.706	6	3.935	6
	Gumbel min	0.125	5	0.900	5	1.716	2	1.942	2

concrete was considered by selecting the recommended distribution as per Table 9. The strength properties of reinforcement steel and other modelling properties were considered at their mean values. Forty-four selected ground motions were linearly scaled to have PGA from 0.1*g* to 1.0*g*. Using the sampling technique 44 different values of concrete compressive strength were generated to create 44 building models. Each of the 44 building models was analysed for one randomly selected ground motion with randomly selected PGA using NLTHA. The demand parameter (ISD) obtained from the NLTHA and the corresponding intensity measure (PGA) are plotted in

Table 10 Recommended variability models for strength properties (MPa) of WCS concrete

mix	compressive strength	flexural strength	split tensile strength
M0	normal (46.25, 0.79)	normal (5.22, 0.26)	normal (3.87,0.22)
M20	Gumbel max (45.96, 0.77)	Gamma (388.56, 0.02)	Gumbel max (3.89, 0.16)
M40	Gumbel max (47.14, 1.15)	Gumbel min (5.52, 0.20)	normal (4.3, 0.198)
M60	Gumbel max (50.89,1.15)	Gamma (517.6, 0.01)	normal (4.33, 0.18)
M80	normal (53.86, 2.56)	Gumbel min (5.93, 0.17)	Gumbel max (4.31,0.15)
M100	normal (46.01, 0.94)	normal (5.23, 0.27)	Weibull (23.83, 4.20)

Note: Values in parenthesis present shape and scale parameters for each distribution

Fig. 7. The power-law relation between ISD and PGA was developed through regression analysis, which represented PSDMs for the selected building. A higher value of ISD corresponded to the higher vulnerability of the building. It can be seen from Fig. 7 that no significant change in the ISD was observed for the building frame modelled with WCS concrete as compared to the control mix (M0). The fragility curves were developed for the selected building at the chosen performance limit states, as shown in Fig. 8.

It can be seen from Fig. 8 that the percentage replacement of WCS did not change the fragility curves of the selected building substantially which was in agreement with the results of PSDMs. The building modeled with 100% replacement of WCS was found to be the most fragile among the considered models although the differences were very small. The order of the building models in terms of increasing probability of failure was found to be M80 < M60 < M40 < M20 ≤ M0 < M100, which follows the hierarchy of mean compressive strength as evident from Table 3. These results confirm that the WCS concrete can be used in seismic resistant structures safely as WCS results in an identical probability of failure and dispersion in the drift demand when compared with the conventional concrete building.

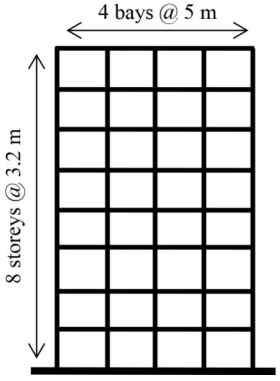

Fig. 6 Geometry of the selected RC frame.

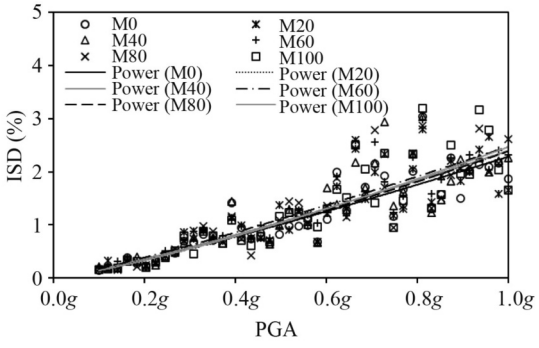

Fig. 7 PSDMs for WCS incorporated RC frames.

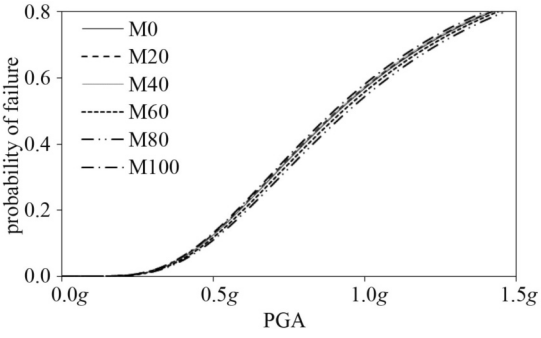

Fig. 8 Fragility curves for WCS incorporated RC frames.

6 Conclusions

The use of WCS as an alternative to natural sand can bring increased sustainability to concrete construction by utilizing waste and conserving natural resources. However, the utilization of WCS in the construction industry is low. This paper aims to build confidence among the stakeholders by providing research output on the behavior of both concrete and structure incorporating WCS. The paper addresses two important aspects: (i) modeling the strength uncertainty of WCS concrete required to formulate the limit state and reliability- based design and (ii) the performance of WCS concrete in seismically resistant RC framed buildings.

Quantification of uncertainty associated with the strength of WCS concrete was investigated and the best-fit distribution functions that perform well in describing the variability in different strength properties of WCS concrete are recommended. The information of variability

in the strength properties is essential for the formulation of limit-state design and safety assessment of structures made of WCS concrete. It is to be noted here that construction at a practical site may have additional variability resulting from raw materials obtained from different sources, different climatic conditions, differences in quality control, etc., which are not included in the present study.

Seismic risk of a selected RC framed building incorporating various dosages of WCS as fine aggregate was assessed using an accepted probability-based methodology. Estimated seismic risk, in terms of PSDM and fragility curve, shows that WCS concrete results in an identical probability of failure and dispersion in the drift demand when compared with the conventional concrete made of natural sand. Therefore, it can be concluded that WCS concrete will create seismic resistance similar to that of conventional concrete in RC framed buildings.

References

1. Paris J M, Roessler J G, Ferraro C C, de Ford H D, Townsend T G. A review of waste products utilized as supplements to Portland cement in concrete. Journal of Cleaner Production, 2016, 121: 1−18
2. Shah S N, Mo K H, Yap S P, Yang J, Ling T C. Lightweight foamed concrete as a promising avenue for incorporating waste materials: A review. Resources, Conservation and Recycling, 2021, 164: 105103
3. Kirthika S K, Singh S K, Chourasia A. Alternative fine aggregates in production of sustainable concrete—A review. Journal of Cleaner Production, 2020, 268: 122089
4. Dash M K, Patro S K, Rath A K. Sustainable use of industrial-waste as partial replacement of fine aggregate for preparation of concrete—A review. International Journal of Sustainable Built Environment, 2016, 5(2): 484−516
5. Tavakoli D, Hashempour M, Heidari A. Use of waste materials in concrete: A review. Pertanika Journal of Science & Technology, 2018, 26(2): 499−522
6. Collivignarelli M C, Cillari G, Ricciardi P, Miino M C, Torretta V, Rada E C, Abbà A. The production of sustainable concrete with the use of alternative aggregates: A review. Sustainability, 2020, 12(19): 7903
7. Zhang X, Li W, Tang Z, Wang X, Sheng D. Sustainable regenerated binding materials (RBM) utilizing industrial solid wastes for soil and aggregate stabilization. Journal of Cleaner Production, 2020, 275: 122991
8. Mistri A, Bhattacharyya S K, Dhami N, Mukherjee A, Barai S V. Petrographic investigation on recycled coarse aggregate and identification the reason behind the inferior performance. Construction & Building Materials, 2019, 221: 399−408
9. Kisku N, Joshi H, Ansari M, Panda S K, Nayak S, Dutta S C. A critical review and assessment for usage of recycled aggregate as sustainable construction material. Construction & Building Materials, 2017, 131: 721−740
10. Al-Jabri K S, Hisada M, Al-Saidy A H, Al-Oraimi S K. Performance of high strength concrete made with copper slag as a fine aggregate. Construction & Building Materials, 2009, 23(6): 2132−2140
11. Shi C, Meyer C, Behnood A. Utilization of copper slag in cement and concrete. Resources, Conservation and Recycling, 2008, 52(10): 1115−1120
12. Arino A M, Mobasher B. Effect of ground copper slag on strength and toughness of cementitious mixes. ACI Materials Journal, 1999, 96(1): 68−73
13. Tixier R, Devaguptapu R, Mobasher B. The effect of copper slag on the hydration and mechanical properties of cementitious mixtures. Cement and Concrete Research, 1997, 27(10): 1569−1580
14. Moura W A, Gonçalves J P, Lima M B L. Copper slag waste as a supplementary cementing material to concrete. Journal of Materials Science, 2007, 42(7): 2226−2230
15. Gorai B, Jana R K, Premchand. Characteristics and utilization of copper slag—A review. Resources, Conservation and Recycling, 2003, 39(4): 299−313
16. Al-Jabri K S, Al-Saidy A H, Taha R. Effect of copper slag as a fine aggregate on the properties of cement mortars and concrete. Construction & Building Materials, 2011, 25(2): 933−938
17. Wu W, Zhang W, Ma G. Optimum content of copper slag as a fine aggregate in high strength concrete. Materials & Design, 2010, 31(6): 2878−2883
18. Alnuaimi A S. Effects of copper slag as a replacement for fine aggregate on the behavior and ultimate strength of reinforced concrete slender columns. Journal of Engineering Research, 2012, 9(2): 90−102
19. Murari K, Siddique R, Jain K K. Use of waste copper slag, a sustainable material. Journal of Material Cycles and Waste Management, 2015, 17(1): 13−26
20. Ambily P S, Umarani C, Ravisankar K, Prem P R, Bharatkumar B H, Iyer N R. Studies on ultra-high performance concrete incorporating copper slag as fine aggregate. Construction & Building Materials, 2015, 77: 233−240
21. Mavroulidou M. Mechanical properties and durability of concrete with water cooled copper slag aggregate. Waste and Biomass Valorization, 2017, 8(5): 1841−1854
22. Zaidi K A, Ram S, Gautam M K. Utilization of glass powder in high strength copper slag concrete. Advances in Concrete Construction, 2017, 5(1): 65−74
23. Raju S, Dharmar B. Durability characteristic of copper slag concrete with fly ash. Gradevinar, 2017, 69(11): 1031−1040
24. Thomas J, Thaickavil N N, Abraham M P. Copper or ferrous slag as substitutes for fine aggregate in concrete. Advances in Concrete Construction, 2018, 6(5): 545−560
25. Nowak A S, Collins K R. Reliability of Structures. New York: McGraw-Hill, 2000
26. Kilinc K, Celik A O, Tuncan M, Tuncan A, Arslan G, Arioz O. Statistical distributions of *in-situ* micro core concrete strength. Construction & Building Materials, 2012, 26(1): 393−403
27. Campbell R H, Tobin R E. Core and cylinder strengths of natural and lightweight concrete. Journal of Materials in Civil

Engineering, 1967, 64(4): 190−195
28. Soroka I. An application of statistical procedures to quality control of concrete. Materiales de Construcción, 1968, 1(5): 437−441
29. Chmielewski T, Konopka E. Statistical evaluations of field concrete strength. Magazine of Concrete Research, 1999, 51(1): 45−52
30. Graybeal B, Davis M. Cylinder or cube: Strength testing of 80 to 200 MPa (11. 6 to 29 ksi) ultra-high-performance fiber-reinforced concrete. ACI Materials Journal, 2008, 105(6): 603−609
31. Chen X, Wu S, Zhou J. Variability of compressive strength of concrete cores. Journal of Performance of Constructed Facilities, 2014, 28(4): 06014001
32. Pacheco J, De Brito J, Chastre C, Evangelista L. Experimental investigation on the variability of the main mechanical properties of concrete produced with coarse recycled concrete aggregates. Construction & Building Materials, 2019, 201: 110−120
33. Sahoo K, Dhir P K, Teja P R R, Sarkar P, Davis R. Variability of silica fume concrete and its effect on seismic safety of reinforced concrete buildings. Journal of Materials in Civil Engineering, 2020, 32(4): 04020024
34. Sahoo K, Kumar Dhir P, Teja P R R, Sarkar P, Davis R. Seismic safety assessment of buildings with fly-ash concrete. Practice Periodical on Structural Design and Construction, 2020, 25(3): 04020024
35. ASTM. Standard Specification for Portland Cement, ASTM C150/C150M. West Conshohocken, PA: ASTM, 2019
36. ASTM. Standard Specification for Concrete Aggregates, ASTM C33/C33M. West Conshohocken, PA: ASTM, 2018
37. Panda S, Sarkar P, Davis R. Abrasion resistance and slake durability of copper slag aggregate concrete. Journal of Building Engineering, 2021, 35: 101987
38. ASTM. Standard Practice for Making and Curing Concrete Test Specimens in the Laboratory, ASTM C192/C192M. West Conshohocken, PA: ASTM, 2016
39. IS. Method of Tests for Strength of Concrete. Bureau of Indian Standards, IS 516. New Delhi: IS, 1959
40. ASTM. Standard Test Method for Splitting Tensile Strength of Cylindrical Concrete Specimens, ASTM C496. West Conshohocken, PA: ASTM, 2017
41. ASTM. Standard Test Method for Flexural Strength of Concrete Specimens, ASTM C293. West Conshohocken, PA: ASTM, 2016
42. Lilliefors H W. On the Kolmogorov-Smirnov test for normality with mean and variance unknown. Journal of the American Statistical Association, 1967, 62(318): 399−402
43. Sahu S, Sarkar P, Davis R. Uncertainty in bond strength of unreinforced fly-ash brick masonry. Journal of Materials in Civil Engineering, 2020, 32(3): 06020003
44. Stephens M A. EDF statistics for goodness of fit and some comparisons. Journal of the American Statistical Association, 1974, 69(347): 730−737
45. Lawrence S J. Random Variations in Brickwork Properties. 7th ed. Melbourne: Brick Masonry Conference, 1985: 537−547
46. Montazerolghaem M. Analysis of unreinforced masonry structures with uncertain data. Dissertation for the Doctoral Degree. Dresden: Dresden University of Technology, 2015
47. Sorrentino L, Infantino P, Liberatore D. Statistical tests for the goodness of fit of mortar compressive strength distributions. In: The 16th International Brick and Block Masonry Conference. Italy: CRC Press, 2016
48. Sahu S, Sarkar P, Davis R. Quantification of uncertainty in compressive strength of fly ash brick masonry. Journal of Building Engineering, 2019, 26: 100843
49. Chandrappa A K, Biligiri K P. Flexural-fatigue characteristics of pervious concrete: Statistical distributions and model development. Construction & Building Materials, 2017, 153: 1−15
50. Forbes C, Evans M, Hastings N, Peacock B. Statistical Distributions. 4th ed. New York: Wiley, 2011
51. EasyFit. Version 5.6. Dnepropetrovsk: MathWave Technologies. 2015
52. Sun D, Wu K, Shi H, Zhang L, Zhang L. Effect of interfacial transition zone on the transport of sulfate ions in concrete. Construction & Building Materials, 2018, 192: 28−37
53. Sun D, Wu K, Shi H, Miramini S, Zhang L. Deformation behavior of concrete materials under the sulfate attack. Construction & Building Materials, 2019, 210: 232−241
54. Sun D, Shi H, Wu K, Miramini S, Li B, Zhang L. Influence of aggregate surface treatment on corrosion resistance of cement composite under chloride attack. Construction & Building Materials, 2020, 248: 118636
55. Cornell C A, Jalayer F, Hamburger R O, Foutch D A. Probabilistic Basis for 2000 SAC Federal Emergency Management Agency Steel Moment Frame Guidelines. Journal of Structural Engineering, 2002, 128(4): 526−533
56. Celik O C, Ellingwood B R. Seismic fragilities for non-ductile reinforced concrete frames—Role of aleatoric and epistemic uncertainties. Structural Safety, 2010, 32(1): 1−12
57. Bhosale A S, Davis R, Sarkar P. Seismic safety of vertically irregular buildings: Performance of existing indicators. Journal of Architectural Engineering, 2018, 24(3): 04018013
58. Haran Pragalath D C, Bhosale A S, Davis R, Sarkar P. Multiplication factor for open ground story buildings: A reliability-based evaluation. Earthquake Engineering and Engineering Vibration, 2016, 15(2): 283−295
59. IS. Indian Standard Criteria for Earthquake Resistant Design of Structures. Part 1 General provisions and buildings. Bureau of Indian Standards, IS 1893. New Delhi: IS, 2016
60. Integrated Software for Structural Analysis and Design. SAP2000. Version 22. Berkeley, CA: Computers and Structures, 2020
61. IS. Plain and Reinforced Concrete—Code of Practice. Bureau of Indian Standards, IS 456, New Delhi: IS 456, 2000
62. McKenna F, McGann C, Arduino P, Harmon J A. Open Sees laboratory. 2018 (Available at the website of OpenSees)
63. Haselton C B, Whittaker A S, Hortacsu A, Baker J W, Bray J, Grant D N. Selecting and scaling earthquake ground motions for performing response-history analyses. In: The 15th World Conference on Earthquake Engineering. Lisbon: Earthquake Engineering Research Institute, 2012: 4207−4217
64. Haran P D C, Davis R, Sarkar P. Reliability evaluation of RC frame by two major fragility analysis methods. Asian Journal of Civil Engineering, 2015, 16(1): 47−66